Numerical Investigation on the Torque Yields of the Darrieus Turbine with Various Deflectors Shape and Distance

Aditia Aulia
Department of Mechanical Engineering, Republic of Indonesia Defense University

Ahmad Syafiq Rofi’i
Department of Mechanical Engineering, Republic of Indonesia Defense University

Muhammad Ferry Fadri
Department of Mechanical Engineering, Republic of Indonesia Defense University

Muhammad Haidar Syarif
Department of Mechanical Engineering, Republic of Indonesia Defense University

他

https://doi.org/10.5109/7326963

出版情報：Evergreen. 11 (4), pp.3290-3298, 2024-12. Interdisciplinary Graduate School of Engineering Sciences, Kyushu University, Japan
バージョン：

Numerical Investigation on the Torque Yields of the Darrieus Turbine with Various Deflectors Shape and Distance

Aditia Aulia[1,*], Ahmad Syafiq Rofi'i[1], Muhammad Ferry Fadri[1], Muhammad Haidar Syarif[1], Gunawan Dwi Haryadi[2], Edy Susanto[3]

[1]Department of Mechanical Engineering, Republic of Indonesia Defense University, IPSC Area, Sentul, Bogor, West Java 16810, Indonesia

[2]Department of Mechanical Engineering, Diponegoro University, Semarang, Central Java 50275, Indonesia

[3]Department of Mechanical Engineering, Institute of Technology PLN, Jakarta Barat 11750, Indonesia

*Author to whom correspondence should be addressed:
E-mail: aditia.aulia@idu.ac.id

(Received January 16, 2024: Revised May 7, 2024: Accepted June 24, 2024).

Abstract: This paper investigates the effects on the torque performance caused by deflectors of the Darrieus turbine. Various deflectors were placed in front of the turbine and disrupted the wind flow before it came into contact with the turbine blades. Using numerical method, this study aims to find the deflector's optimum geometric shape, offset distance, and dimension required for the turbine to produce the highest torque. This study utilizes flow simulation analysis to simulate the deflector effect on Darrieus turbine. The result of this study is the optimum deflector geometry and offset distance for producing highest turbine torque output. From the data gathered it is shown that a deflector with triangular cross-section with the size of turbine diameter placed 400 mm offset to the right of the turbine produces the best result. Turbine with this deflector configuration produces 1.24 Nm of torque, eight times higher than its non-deflector counterpart yields 0.14 Nm.

Keywords: deflector; Darrieus turbine; geometry; offset

1. Introduction

In pursuing the growing demand for clean and sustainable energy sources, wind stands out as a prominent and rapidly expanding sector. Wind as an energy source has had its origin way back in the ancient times. The use of vertical-axis windmills were recorded in the Persian-Afghan borders circa 200 BC, while horizontal-axis windmills appeared much later in the Netherlands and the Mediterranean, between 1300-1875 AD[1]. Wind power has emerged as a highly prevalent and extensively utilized form of renewable energy, with mechanical equipment being employed to convert it into electrical energy[2]. Utilizing wind energy for electricity generation, instead of fossil fuels, has the dual benefit of conserving conventional energy resources and safeguarding the environment[3]. According to the data from International Renewable Energy Agency (IRENA), the global wind energy capacity has increased significantly in the last decade, as shown in Fig. 1[4]. The rate of development and deployment accelerated rapidly in recent years because of its many benefits, such as being cost-effective, reliable, and environmentally friendly[5].

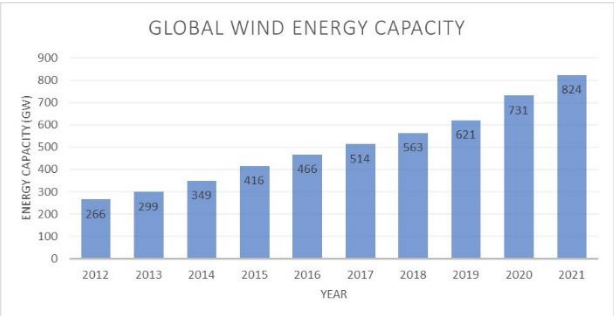

Fig. 1: Global Energy Capacity data[4]

In the present day, numerous countries are allocating a growing amount of funds towards the establishment of wind turbines[6]. Indonesia is one of the leading countries in wind power development in Southeast Asia, with the capacity of 9,861 MW. However, the development of wind power in Indonesia poses some challenges. According to the data from Indonesian Ministry of Energy and Mineral Resources 2020-2024, Indonesia has an average annual wind speed of around 3-6 m/s , only half the capacity of countries located in the northern and southern hemispheres that experience wind speeds greater than 8 m/s. This lower wind speed happens due to Indonesia's geographical condition, which is located on the equator with moderate air temperature and low air pressure[7].

The two most common wind turbine configuration is Horizontal Axis Wind Turbine (HAWT) and Vertical Axis Wind Turbine (VAWT). Horizontal axis wind turbines (HAWT) are the most common type of wind turbine design due to their superior power performance compared to the other[8]. However, HAWTs require substantial space, and the chosen location must have abundant wind energy resources to accommodate their considerable dimensions and address the noise issue at the same time[9]. The VAWT configuration required minimum wind speed of only 2 m/s, which is more suitable to be implemented in Indonesia[7]. Besides that, VAWT exhibit substantial potential in urban settings as they uphold a notable power coefficient[10]. The unique attributes of vertical axis wind turbines render them appropriate for urban settings[11]. In the past few years, there has been rapid development in kilowatt-level VAWTs within urban areas[12]. However, the location of urban installation which have different geometric conditions affect turbine production[13]. The constrained power coefficient poses a limitation on the extensive utilization of VAWTs[14]. Basic types of VAWTs commonly include the H-Rotor type, Darrieus type, and Savonius type[15]. The Darrieus turbine, classified as a lift-type VAWT, possesses the advantage of functioning effectively at low wind speeds[16]. However, it exhibits a drawback in terms of aerodynamic performance when compared to horizontal-axis turbines[17]. Therefore, improvements are needed to increase VAWT efficiency.

Numerous attempts have been undertaken to enhance the power efficiency of VAWTs, such as refining airfoil selection and optimization[18]. Chen et al. found that thickness-chord ratio has a significant influence on the power coefficient[19]. Tavernier et al. compared optimized airfoils of VAWT with reference airfoils from the first generation. The optimized airfoils demonstrate superior performance in power coefficient compared to the reference airfoils[20]. Moreover, the utilization of variable-pitch methods has also been implemented to discover the optimal outcome in power production[21]. The adjustment of the pitch angle represents a prospective factor for improving the performance of VAWT turbines[22]. A vertical axis wind turbine with fixed-pitch straight blades undergoes consistent changes in the wind attack angle as a result of its rotation pattern, resulting in poor power generation. To address the problem, some studies investigated blade pitch control technology, which involves adjusting the pitch angle of a blade to modify the wind attack angle, thereby altering the aerodynamic forces acting on the blade[23].

Some studies focus on minimizing aerodynamic losses[24]. With the advantages of low cost and impressive visualization capabilities, Computational Fluid Dynamics (CFD) technology has prompted a growing number of scholars to explore the aerodynamic traits of wind turbines using this technology[25]. Villenueve et al. investigate the impact of the blade support structures on the performance of a single-blade vertical-axis wind turbine through three-dimensional URANS simulations. The findings indicate that the efficiency of the turbine is greatly influenced by the placement of the struts[26]. Ashwindran et al. conducted research examining how blade geometry influences the airflow interaction with wind. They effectively formulated mathematical methods for shaping blade morphology to impact the drag generated by the turbine[27]. Some modifications applied to improve VAWT performance, including design of the turbine itself, such as airfoil shape and size, tilt angle, and pitch angle.

Meanwhile, some researchers favored the use of augmentation devices such as diffuser, guide vanes, stator, shroud, plate, deflector, or duct to improve the wind turbine efficiency[28]. Incorporating a deflector into the conventional wind turbine system has been identified as the most straightforward approach to augmenting the coefficient of performance while simultaneously mitigating the adverse torque effects induced by the returning blades.[28]. Wong et al. demonstrated that the deflector functioned as a power-enhancing mechanism, leading to an improved performance of the VAWT [29]. In essence, the deflector helps minimize the detrimental effects that can affect the overall efficiency of the wind turbine[30]. This function is important because negative torque can reduce the efficiency of a wind turbine. The deflector serves to direct and concentrate the airflow, aiming to enhance positive torque and diminish negative torque in wind turbines. By employing the deflector, the airflow can be efficiently directed to optimize energy production, amplifying the generated torque while mitigating the negative forces that influence the overall performance of the wind turbine[31]. According to the numerical simulation, Tavernier et al. found that the deflected mass flow contributes to the power enhancement of the double-rotor layout[32].

The study about the effect of deflector on Darrieus turbine that has been conducted in the past, such as that by Zidane et al.[28], uses a deflector plate and variation in the plate angle, while Bachtiar and Ariwiyono[38] only considers the effect of offset distance of a triangular deflector. This paper improves upon previous research by proposing an investigation on the effect of various geometric shapes and sizes of the deflector, as well as its offset distance relative to the turbine. This study utilizes a transient 3D model to compare and optimize the performance of the Darrieus wind rotor by varying the deflector geometry. The primary objective of this research is to determine the optimal shape, size, and offset distance for the deflector, to maximize the torque generated from wind energy. The overarching goal is to uncover a novel approach that can effectively improve the efficiency of Daerrius turbines in the foreseeable future. The results of this research will yield an accurate geometric model that can be implemented in front of Darrieus wind turbines.

2. Methods and Procedures

Within the past decade, the use of computational fluid dynamics (CFD) has grown significantly. CFD simulation can reduce the cost of experiments, as the complex geometries of an engineering design can be modeled. Many research on improving Darrieus turbine's aerodynamic performance by implementing modifications had been conducted. However, the effect of adding deflector and modifying its variables on the turbine's performance was not examined in these works.

The aerodynamic efficiency of the H-Darrieus wind turbine relies on the flow properties surrounding its blades[33]. From this point of view, the present study is focused on suggesting deflectors geometrical impact using the numerical optimization method on the torque yields. The Flow algorithm used Navier-Stokes Equation to solve the flow problem[34] which is an equation of mass, momentum, and energy conservation laws.

$$\frac{\partial \rho}{\partial t} + \frac{\partial(\rho u_i)}{\partial x_i} = 0 \qquad (1)$$

$$\frac{\partial(\rho u_i)}{\partial t} + \frac{\partial}{\partial x_j}\left(\rho u_i u_j\right) + \frac{\partial P}{\partial x_i} = \frac{\partial}{\partial x_j}\left(\tau_{ij} + {\tau_{ij}}^R\right) + S_i \qquad (2)$$

$$\frac{\partial \rho H}{\partial t} + \frac{\partial \rho u_i H}{\partial x_i} = \frac{\partial}{\partial x_j}\left(u_j\left(\tau_{ij} + {\tau_{ij}}^R\right) + q_i\right) + \frac{\partial p}{\partial t} - {\tau_{ij}}^R \frac{\partial u_i}{\partial x_j} + \rho\varepsilon + S_i u_i + Q_H \qquad (3)$$

$$H = h + \frac{u^2}{2} \qquad (4)$$

Here, the term $-\rho uj\,'\,ui\,'$ is the Reynolds stress model, ui is the velocity component, ρ is fluid density, P is fluid pressure, k is turbulent kinetic energy, h is enthalpy, τ is deviatoric stress tensor, ε is the dissipation of turbulent kinetic energy, μ is dynamic viscosity of fluid, Q_H is the amount of heat, μ_t is eddy viscosity, and S is entropy, while i and j is the direction of vector. While where $C\varepsilon 1$ = 1.44, $C\varepsilon 2$ =1.92, $C\mu$ =0.09, σk=1, $\sigma\varepsilon$=1.3, σB =0.9, CB =1, CB =1 if P_B <0 an CB=0 if P_B >0.

The flow simulation modeled turbulence using the modified k-ε model that makes the equations easier to solve. This model consisted of the following turbulence conservation laws:

$$\frac{\partial \rho k}{\partial t} + \frac{\partial \rho k u_i}{\partial x_i} = \frac{\partial}{\partial x_i}\left(\left(\mu + \frac{\mu_t}{\sigma_k}\right)\frac{\partial k}{\partial x_i}\right) + {\tau_{ij}}^R \frac{\partial u_i}{\partial x_j} - \rho\varepsilon + \mu_i P_B \frac{\partial \rho\varepsilon}{\partial t} + \frac{\partial \rho\varepsilon u_i}{\partial x_i} = \frac{\partial}{\partial x_i}\left(\left(\mu + \frac{\mu_i}{\sigma_i}\right)\frac{\partial k}{\partial x_i}\right) + C_{\varepsilon 1}\frac{\varepsilon}{k}\left(f_1 {\tau_{ij}}^R \frac{\partial u_i}{\partial x_j} + C_B \mu_t P_B\right) - f_2 C_{\varepsilon 2}\frac{\rho\varepsilon^2}{k} \qquad (5)$$

$$\tau_{ij} = \mu S_{ij}, {\tau_{ij}}^R = \mu_i S_{ij} - \frac{2}{3}\rho k \delta_{ij}, S_{ij} = \frac{\partial u_i}{\partial x_j} + \frac{\partial u_j}{\partial x_i} - \frac{2}{3}\delta_{ij}\frac{\partial u_k}{\partial x_k}, \qquad (6)$$

$$P_B = -\frac{g_i}{\sigma_B}\frac{1}{\rho}\frac{\partial \rho}{\partial x_i} \qquad (7)$$

The turbine design used in this study is NACA 4415 airfoil. Four different shapes of deflector cross section are tested in this simulation, which are circle, rectangle, triangle, and diamond. The deflector is installed at the front of the turbine and placed offset to the right. This configuration aims to increase the torque produced by the turbine and this study's goal is to find the optimum deflector cross section shape and distance from the turbine. The inlet works as an incoming wind velocity with velocity of around 4.5 m/s. This condition is chosen as the middle ground from Indonesia average wind speed of 3-6 m/s taken from the data of the Ministry of ESDM and Global Wind Atlas at the height of 10 m. The wall works as a smooth wall so that the wake induced by the wall can be neglected, and the outlet works as wind exit that has pressure of 101325 Pa. The turbulence model in this study are modeled using the modified k-ε model. The schematic of this setup can be seen in Fig. 2.

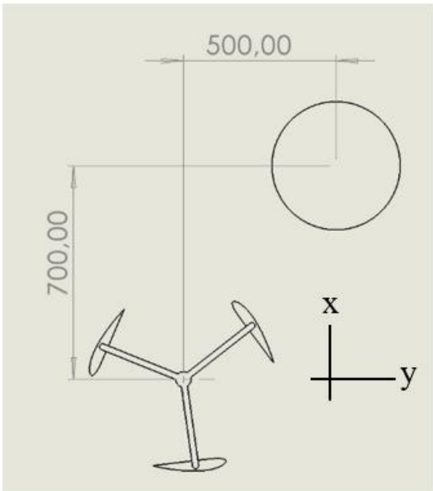

(a)

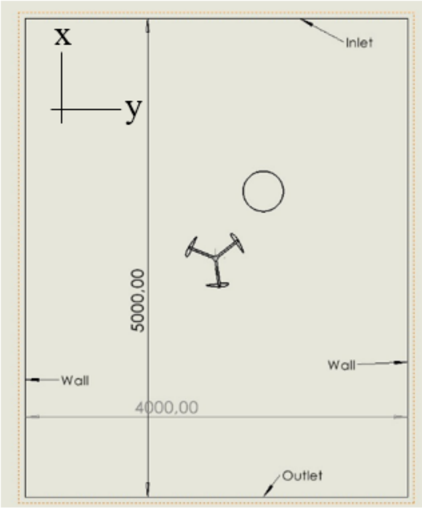

(b)

Fig.2: The schematic setup for: (a) Simulation setup with circle deflector, and (b) Boundary condition setup.

This study runs multiple simulations on every case. The data is collected from each shape of the deflector, each size of the deflector, and offset distance variation. The x-distance of 700 mm was chosen as the independent variable. In this study, torque produced by the turbine with each of the four shapes of deflector are compared. For each shape, the simulation runs between the offset distance y of 0 to 500 mm with 100 mm increments, and for every 100 mm the diameter of the deflector was varied from 0,1 to 1 times of the turbine diameter DT. The shape and geometry of deflectors and 3D model of the turbine is shown in the Fig. 3.

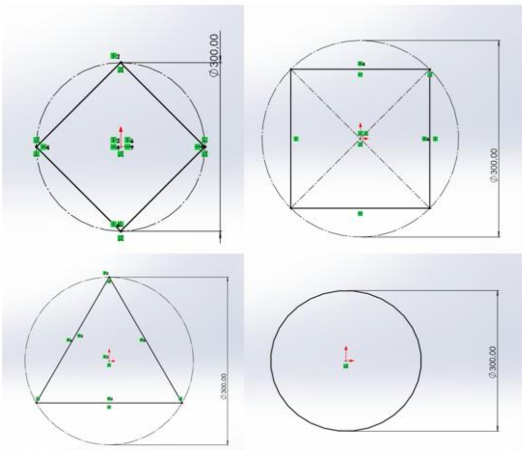

(a)

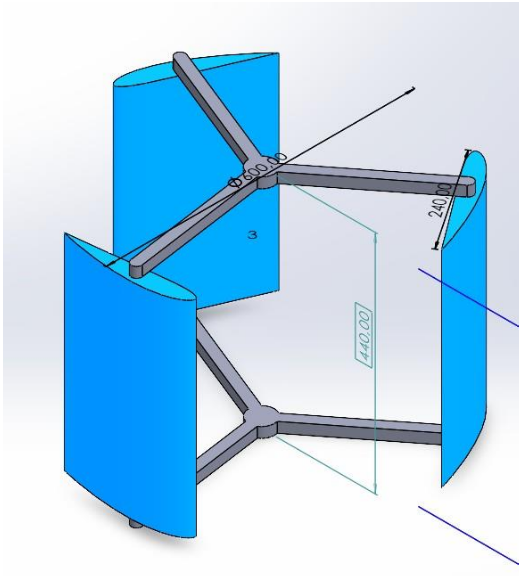

(b)

Fig. 3: (a) Deflectors shape and geometry, and (b) 3D model of the turbine.

The flow simulation is based on immersed body mesh approach. Mesh consists of adjacent rectangular cells that extend to the computational domain's external boundary. In this approach the generation of the mesh starts independently from the body itself and the cells can easily intersect the boundary between solid and fluid. The benefit of this mesh approach is make the simulation more simple, fast, and robust, with minimal local truncation errors and improve robustness with differential schemes[31]. The mesh schematic of the simulation is shown in Fig. 4.

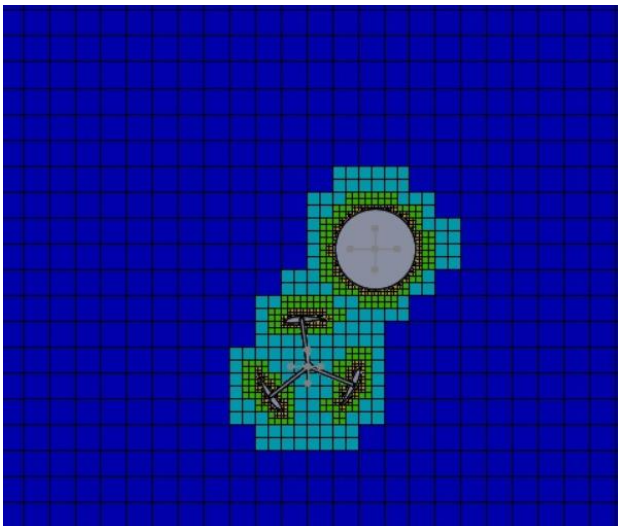

(a)

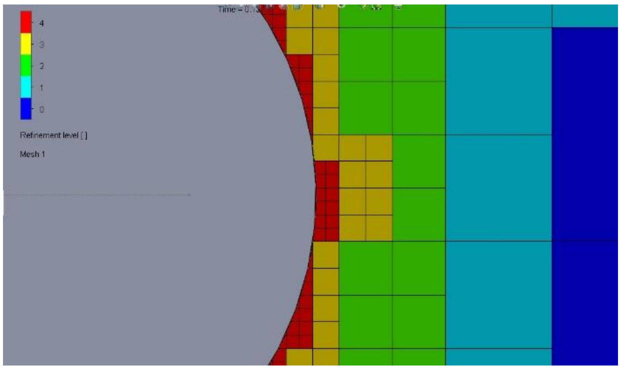

(b)

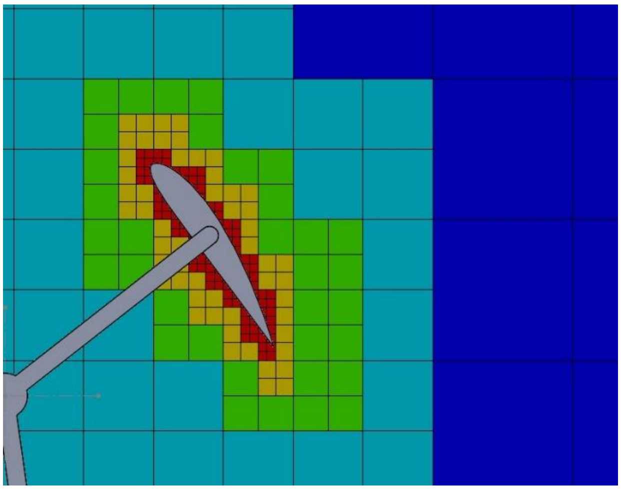

(c)

Fig. 4: (a) Mesh domain for the simulation, (b) Close up view of the mesh on deflector, (c) Close up view of the mesh on the blade

Given the need to conduct multiple simulations, an automatic global meshing method was employed. This approach enabled the collection of data that was both highly accurate and efficient, thereby maximizing the potential of the available resources.

In order to evaluate the mesh's influence on the simulation results, grid independence test is performed. After the data from the first mesh is extracted, the mesh is refined before the second simulation runs. This process is repeated until the result of the simulation found to be or nearly similar as the previous ones[39]. Five mesh level is tested to obtain the torque data on every mesh level. Figure 5 below shows the amount of torque on every mesh level. It can be seen that mesh level 3 and 4 yield almost similar result with difference of approximately 2.46%. Therefore, it is decided to use level 4 mesh for the simulation.

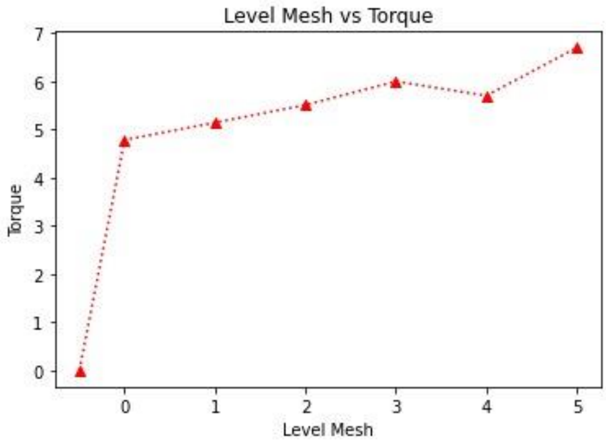

Fig. 5: Grid independency results

To verify the results, the mass flow rate change between the inlet and outlet is measured. As shown in Fig. 6 the mass flow rate difference between input and output is very small, which verified that the simulations are correct.

Goal Name	Unit	Value
SG Mass Flow Rate Output	[kg/s]	-64.2441614
SG Mass Flow Rate Input	[kg/s]	64.24416087
Equation Goal 1	[kg/s]	-5.6123E-07

Fig. 6: Mass flow rate verification

3. Results and Discussion

The simulations were performed for all types of cross-sectional shapes of the deflector. For each cross-sectional shape, the offset distance of the deflector was varied, and for every distance the diameter of the deflector was varied. These variations affect the flow characteristics flowing through the turbine. The flow characteristics around the blade significantly influence the aerodynamic performance of the H-Darrieus wind turbine[35]. The offset distance ranged from 0-500 mm in 100 mm increments, while the diameter ranged from 0.1 to 1 time the turbine diameter. The author choose offset distance range for a specific reason. The deflector's effect decreases after 300mm, so continuing the simulation with a further distance can result in the turbine generating the same amount of torque as a non-deflector turbine. Based on previous simulations conducted by the authors, a 700mm x-axis offset has been chosen. The simulations indicated that increasing the x-axis offset number results in decreased torque production by the turbine, and negative torque may even occur at certain points. On the other hand, if the offset is less than 700mm, the blade could potentially collide with the deflector during rotation. The torque performance curves as the function of each shape of the deflector is shown in Fig. 7. It is observed from the graph that the increase in diameter of the deflector results in increasing the dynamic torque. However, we observe that using the deflector, the turbine has higher torque compared to the non-deflector turbine. At peak level, the increase is significant at around 50%. It is evident that with increasing diameter of the deflectors, The area behind the deflector and the turbine's wake become less turbulent.

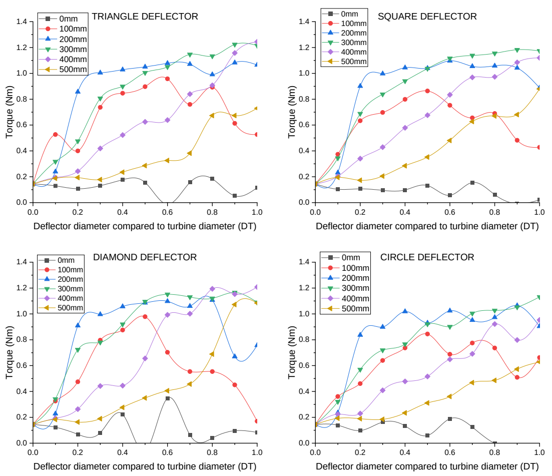

Fig. 7: The torque performance curves as the function of each shape of the deflector.

It can be seen from the results that some distances can lead to a decrease in torque at a certain diameter. The Darrieus turbine rotates with the help of lift force. Besides the lift force, the airfoil on each blade produces drag force. The diagram of the force acting on the turbine is shown in the Fig. 8a. Figure 8b shows wind flow illustration with triangle deflector. From Figure 8, blade number 1 generates negative torque. To overcome this condition, the deflector is added offset to the right to decrease wind velocity around blade number 1 by blocking the wind flow from impacting blade number 1 and increase the velocity around other blades by deflecting the wind flow, and at the same time decrease the amount of negative torque and increasing the positive torque generated by the turbine. Therefore, the net torque of the turbine increases. In the case of negative net torque, the disruption of the wind flow caused by the deflector also decrease the wind velocity on blade number 2. This is why negative net torque usually happens at 0 mm offset distance y where the wind velocity on both blade number 1 and blade number 2 are low.

The highest torque produced by the turbine for each deflector shape are as follows: 1.13 Nm for the cylinder at 300 mm distance with the size of turbine diameter, 1.20 Nm for the diamond at 400 mm distance and with the size of turbine diameter, 1.17 Nm for square at 300 mm distance with the size of turbine diameter, and 1.24 Nm for the triangle at 400 mm distance with the size of turbine diameter. Performance comparisons between deflector shapes are shown in the Fig. 9.

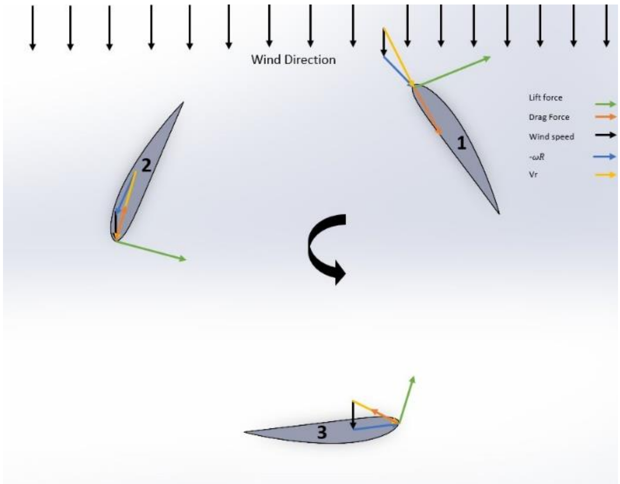

(a)

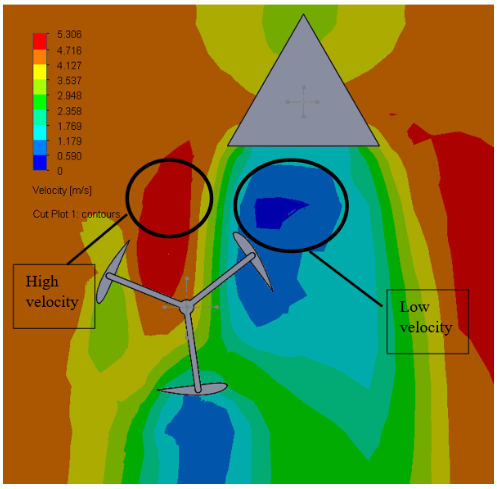

(b)

Fig. 8: (a) Force diagram acting on the turbine, (b) Wind flow around the turbine with triangular deflector.

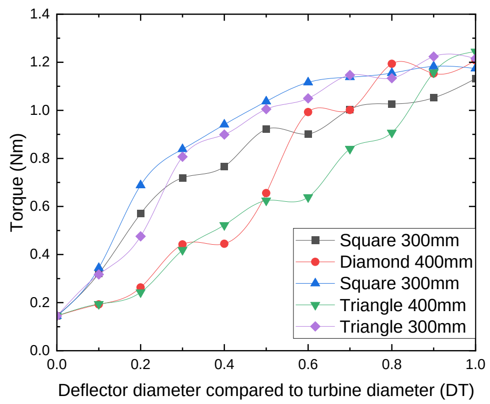

Fig. 9: Maximum torque produced by each deflector with optimum distance.

From Figure 9, it can be seen that when the diameter of the deflector is between 0.1 and 0.6 DT, the highest torque was produced by the square deflector, whereas between 0.7 and 1 DT, the highest torque produced varies between triangle and diamond. What we need to notice is that each shape gives a positive increase in torque produced by the turbine. Based on the maximum torque values, the triangular deflector demonstrates the highest torque at 1.24 Nm, followed by the diamond deflector with a value of 1.20 Nm. Conversely, the circular and square deflectors exhibit lower maximum torque values. Based on these considerations, the triangular deflector achieves a combination of high maximum torque and relatively low minimum torque. Consequently, among the four provided deflector types, the triangular deflector is deemed the most optimal in torque generation based on the available data. With a triangular deflector, the turbine produces torque eight times higher than its non-deflector counterpart.

The triangular deflector utilizes a uniform distribution of air pressure across its surface. Pressure can vary on a triangular shape depending on the angle and geometry of the triangle. Generally, the pressure is higher on the steeper or sharper sides of the triangle and lower on the more gentle or curved sides. By capitalizing on this principle, the triangular deflector maintains airflow stability around it, avoiding turbulence that can decrease torque efficiency. With its evenly distributed pressure, the triangular deflector generates consistent and strong torque, positively impacting the overall performance of the turbine[36]. In addition, the presence of deflector resulting in velocity change around the turbine blade. The velocity of the turbine also has an influence on the turbulent kinetic energy generation[37]. The idea of this deflector design on Darrieus turbine is advantageous technically for optimizing the torque yields in the power generation fields.

The performance of the deflector-equipped turbine only relies on the shape and size of the deflector. Therefore, the deflector can be manufactured using any material as long as the shape and size are correct. This condition creates an opportunity for recycled material to be used to make the deflector and any existing turbine can be easily modified without having to make an entirely new turbine design.

4. Conclusions

Adding a deflector in front of a Darrieus VAWT (Vertical Axis Wind Turbine) can significantly enhance the turbine's torque output. The deflector redirects the airflow towards the turbine blades, leading to an amplified lift force and thereby increasing the torque output. The effectiveness of the deflector depends on its shape, with a triangular deflector proving to be the most efficient. It concentrates the airflow towards the turbine blades, optimizing their performance. The recommended configuration involves positioning the deflector at an offset distance y of 400 mm, with a diameter matching that of the turbine.

In this study, the highest torque output was achieved with a triangular deflector positioned offset 400 mm to the right of the turbine and having the same diameter as the turbine. The resulting torque output of 1.24 Nm was eight times greater than that of a turbine without a deflector which produced a torque of 0.14 Nm. The study utilized a computational fluid dynamics (CFD) model to simulate the Darrieus VAWT. Wind speed was set at 4.5 m/s, and the wind direction corresponded to the negative x-direction. The findings indicate that incorporating a deflector into a Darrieus VAWT constitutes a highly effective approach for maximizing torque yields. This advancement holds great promise for turbines employed in electricity generation or powering other machinery.

Acknowledgment

This research work is supported by Republic of Indonesia Defense University in collaboration with Diponegoro University and Institute of Technology PLN.

References

1) J. K. Kaldellis, and D. Zafirakis, “The wind energy (r)evolution: A short review of a long history,” Renew. Energy 36(7), 1887–1901 (2011). doi:10.1016/j.renene.2011.01.002.
2) A.M.M. Ismaiel, and S. Yoshida, "Study on Turbulence Intensity Effect on the Fatigue Lifetime on Wind Tubines," Evergreen, 5(1) 25-32 (2018). https://doi.org/10.5109/1929727.
3) H. Meng, M. Wang, O. Olumayegun O, X. Luo, and X. Liu “Process design, operation and economic evaluation of compressed air energy storage (CAES) for wind power through modelling and simulation,” Renew Energy 2019;136:923–36. doi: 10.1016/j.renene.2019.01.043.
4) A. Lebedys, D. Akande, N. Coënt, N. Elhassan, G. Escamilla, I. Arkhipova and A. Whiteman, “Renewable Energy Statistics 2022,” The International Renewable Energy Agency. https://www.irena.org/publications/2022/Jul/Renewable-Energy-Statistics-2022.
5) G. Olabi, K. Obaideen, M. A. Abdelkareem, M. N. AlMallahi, N. Shehata, A. H. Alami, A. Mdallal, A. A. Hassan, and E. T. Sayed, “Wind Energy Contribution to the Sustainable Development Goals: Case Study on London Array,” Sustainability 2023, 15(5), 464. doi:10.3390/su15054641.
6) M. Ghasemian, Z.N. Ashrafi, and A. Sedaghat, “A review on computational fluid dynamic simulation techniques for Darrieus vertical axis wind turbines,” Energy Convers Manage 2017;149:87–100. doi:10.1016/j.enconman.2017.07.016
7) T. Hidayat, "Wind Power in Indonesia: Potential, challenges, and current technology overview," BRIN

Publishing., 109-132 (2022). doi: 10.55981/brin.562.c7.

8) A. M. Halawa, B. Elhadidi, and S. Yoshida, "Aerodynamic Performance Enhancement Using Active Flow Control on DU96-W-180 Wind Turbine Airfoil," Evergreen, 5(1) 16-24 (2018). https://doi.org/10.5109/1929723.

9) H.Y. Peng, H.F. Lam, and H.J. Liu, "Power performance assessment of h-rotor vertical axis wind turbines with different aspect ratios in turbulent flows via experiments," Energy 173 (2019) 121-132. doi:10.1016/j.energy.2019.01.140.

10) M. Maizi, M. Mohamed, R. Dizene, and M. Mihoubi "Noise reduction of a horizontal wind turbine using different blade shapes," Renew Energy. 2018;117:242–56. doi:10.1016/j.renene.2017.10.058

11) F. Balduzzi, A. Bianchini, E.A Carnevale, L. Ferrari, S. Magnani, "Feasibility analysis of a Darrieus vertical-axis wind turbine installation in the rooftop of a building," Appl Energ 2012;97:921–9. doi:10.1016/j.apenergy.2011.12.008

12) R. Kumar, K. Raahemifar, and A.S. Fung, "A critical review of vertical axis wind turbines for urban applications," Renew. Sustain. Energy Rev. 2018;89:281–91. doi:10.1016/j.rser.2018.03.033

13) L. Battisti, E. Benini, A. Brighenti, S. Dell'Anna, and M.R. Castelli, "Small wind turbine effectiveness in the urban environment," Renew Energ 2018;129:102–13. doi: 10.1016/j.renene.2018.05.062.

14) N. Ma, H. Lei , Z. Han, D. Zhou, Y. Bao, K. Zhang, L. Zhou, and C. Chen, "Airfoil optimization to improve power performance of a high-solidity vertical axis wind turbine at a moderate tip speed ratio," Energy 2018;150:236–252. doi:10.1016/j.energy.2018.02.115.

15) H. Lei, D. Zhou D, Y. Bao, Y. Li, and Z. Han, "Three-dimensional improved delayed detached Eddy simulation of a two-bladed vertical axis wind turbine," Energy Conversion Management 2017;133:235-48. doi: 10.1016/j.enconman.2016.11.067.

16) I. Hashem, and M.H. Mohamed, "Aerodynamic performance enhancements of H-rotor Darrieus wind turbine," Energy 2018;142:531–45. doi: 10.1016/j.energy.2017.10.036.

17) M. A. Al-Rawajfeh and M. R. Gomaa, "Comparison between horizontal and vertical axis wind turbine" Intl. Jour. of Appl. Pwr. Eng. 12(1), 13-23 (2023). doi:10.11591/ijape.v12.i1.pp13-23.

18) Y. Wang, S. Shen, G. Li, D. Huang, and Z. Zheng, "Investigation on aerodynamic performance of vertical axis wind turbine with different series airfoil shapes," Renew Energ 2018;126:801–18. doi: doi.org/10.1016/j.renene.2018.02.095.

19) J. Chen, L. Chen, H. Xu, H. Yang, C. Ye, and D. Liu, "Performance improvement of a vertical axis wind turbine by comprehensive assessment of an airfoil family," Energy 2016; 114:318–31. doi: 10.1016/j.energy.2016.08.005.

20) D. De Tavernier, C. Ferreira, and G. Bussel, "Airfoil optimisation for vertical-axis wind turbines with variable pitch," Wind Energy 2019;22(4):547–62. doi: 10.1002/we.2306.

21) C. Li, Y. Xiao, Y.L Xu, Y.X Peng, G. Hu, and S. Zhu, "Optimization of blade pitch in H-rotor vertical axis wind turbines through computational fluid dynamics simulations," Appl Energ 2018;212:1107–25. doi:10.1016/j.apenergy.2017.12.035.

22) A. Rezaeiha, I. Kalkman, B. Blocken, "Effect of pitch angle on power performance and aerodynamics of a vertical axis wind turbine," Appl Energ 2017; 197:132–50. doi:10.1016/j.apenergy.2017.03.128.

23) Y.L. Xu, Y.X Peng, and S. Zhan, "Optimal blade pitch function and control device for high-solidity straight-bladed vertical axis wind turbines," Appl Energ 2019; 242:1613–1625. doi:10.1016/j.apenergy.2019.03.151.

24) W. Hao, H. Mao, S. Lyu, and C. Li, "Study on aerodynamic load reduction and efficiency improvement of VAWT based on DTEF," Ocean Eng 2022; 260: 111966. doi:10.1016/j.oceaneng.2022.111966.

25) Y. Li, S. Yang, F. Feng, and K. Tagawa, "A review on numerical simulation based on CFD technology of aerodynamic characteristics of straight-bladed vertical axis wind turbines," Energ Report 2023; 9: 4360–4379. doi:10.1016/j.egyr.2023.03.082.

26) T. Villeneuve, G. Winckelmans, and G. Dumas, "Increasing the efficiency of vertical-axis turbines through improved blade support structures," Renew Energ 2021;169: 1386–1401. doi:10.1016/j.renene.2021.01.092.

27) S.N. Ashwindran, A.A. Azizuddin, and A.N. Oumer, "Study of $\sqrt{2}$ Conjecture in the Construction of Drag Induced Wind Turbine Blade Morphology," Evergreen, 8(3) 574-585 (2021). https://doi.org/10.5109/4491649.

28) I.F. Zidane, H. M. Ali, G. Swadener, Y. A. Eldrainy, and A. I. Shehata, "Effect of upstream deflector utilization on H-Darrieus wind turbine performance: An optimization study," Alex. Eng. J. 63, 175–189 (2023). doi:10.1016/j.aej.2022.07.052.

29) K.H Wong, W.T. Chong, N.L Sukiman, Y.C. Shiah, S.C. Poh, K. Sopian, and W.C Wang, "Experimental and simulation investigation into the effects of a flat plate deflector on vertical axis wind turbine," Energy Convers Manage 2018;160:109–25. doi:10.1016/j.enconman.2018.01.029.

30) I. F. Zidane, K. M. Saqr, G. Swadener, X. Ma, and M. F. Shehadeh, "On the role of surface roughness in the aerodynamic performance and energy conversion of horizontal wind turbine blades: a review," Int. J. Energy Res. 40(15), 2054–2077 (2016). doi:10.1002/er.3580.

31) I. F. Zidane, Swadener, G. Swadener, X. Ma, M. F. Shehadeh, M. H. Salem, and K. M. Saqr, "Performance of a wind turbine blade in sandstorms using a CFD-BEM based neural network," Jour. of Renew. and Sustain. Energ 2020; 12: 053310. doi:10.1063/5.0012272.
32) D. De Tavernier, C. Ferreira, A. Li, U.S. Paulsen, and H.A. Madsen, "Towards the understanding of vertical-axis wind turbines in double-rotor configuration," Journal of Physics: Conference Series 2018; 1037:022015. doi:10.1088/1742-6596/1037/2/022015.
33) A.M.M. Ismaiel, S.M. Metwalli, B.M.N. Elhadidi, and S. Yoshida, "Fatigue Analysis of an Optimized HAWT Composite Blade," Evergreen, 4 (2/3) 1-6 (2017). https://doi.org/10.5109/1929656.
34) A. Sobachkin, and G. Dumnov, "Numerical Basis of CAD-Embedded CFD," Dassault Systèmes. https://www.solidworks.com/sw/numerical-basis-cad-embedded-cfd-confirmation.htm
35) M.H. Gunel, and H.E Ilgin, "Tall Buildings: Structural Systems and Aerodynamic Form," Routledge Taylor and Francis Group. doi:10.13140/2.1.2658.4002.
36) I. Yaningsih, D.D.D.P Tjahjana, E.P. Budiana, M. Muqoffa, Z. Arifin, Suyitno, K. Enoki, and T. Miyazaki, "Numerical study on the Effect of Rectangular and Triangular Counter-Rotating Vortex Generators on the H-Rotor Wind Turbine Performance," Evergreen, 10(1) 230-241 (2023). https://doi.org/10.5109/6781073.
37) Bachtiar, N. Ariwiyono, "Studi Numerik Pengaruh Perubahan Obstacle Segitiga Terpasang di Depan Returning Blade Terhadap Kinerja Darrieus Wind Turbine Tipe NACA 0015", Jurnal Inovtek Polbeng, 9(1) 79-84 (2019). https://doi.org/10.35314/ip.v9i1.905
38) S.A.H Nassir, F.M. Zawawi, M.Z. Mazlan, S. Samion, M.A.W.M Yazid, U. Abidin, "Numerical Investigation of Wake Energy Induced by Cruising Passenger Vehicles on Highway", Jour. of Adv. Res. in Fluid Mech. and Thermal Sci., 57(2) 175-185 (2019).